Original technical Article

Study on the Dynamic Influence of the Distribution of Cutting Depth on the Ground Surface Quality in a Precision Grinding Process

Yong Chen [a,*], Chao Jiang [b], Xun Chen [b], Guoqin Huang [b] and Zhongwei Hu [b]

[a] College of Mechanical Engineering and Automation, Huaqiao University, Xiamen, 361021, China

[b] Institute of Manufacturing Engineering, Huaqiao University, Xiamen, 361021, China

[c] General Engineering Research Institute, Liverpool John Moores University, Liverpool L3 3AF, U.K

Abstract: Focusing on the excitation mechanisms of self-excited vibration and forced vibration, a time-delay differential model of the radial cutting depth of a single active abrasive grit is presented. Based on the principle of the layered superposition characteristics of each component of radial cutting depth, a full discrete simulation technology is used to analyze the dynamic mechanisms of different vibration excitations on the grinding characteristics. The reliability of the dynamic mechanisms is verified by the corresponding grinding experiments. The verification results demonstrate that static and dynamic components in the grinding dynamics, including radial cutting depth, grinding force, surface roughness and surface morphology of workpiece are greatly influenced by total material removal rate, followed by speed ratio and grinding directions. With the increase of cutting depth, the variation amplitude of grinding process influenced by forced-vibration mechanism are nearly twice larger than those influenced by self-excited vibration mechanism. When speed ratio reduces to a half, surface roughness of workpiece improves by nearly 33 %. The stability of machining process and finish surface of workpiece during up-grinding are better than those during down-grinding, where force reduction by up to 10 % and surface finish improvement by 37 %.

Key words: cutting depth, precision grinding, regenerative vibration, forced vibration, surface morphology, full discrete simulation technology

1. Introduction

Precision grinding is one of primary manufacturing methods that removes materials to acquire surface finish of workpiece on a high accuracy and high-speed stable machine tools. During the grinding, the abrasive grits with different shapes that randomly distributed on the surface of grinding wheel remove workpiece materials [1]. The stability of machining process, the most important key to obtain satisfactory surface finish and quality integrity, continues to be a research hotspot over past few decades [2].

Compared to other machining operations, such as milling, turning and drilling, the material removal mechanism in grinding and the interactions between effective working grits and workpiece are much more complex to characterized accurately due to randomly positioned character of abrasive grits (i.e. the distribution of instantaneous cutting depth of grits) on the circumference of a grinding wheel. The instantaneous cutting depth of single active grit, commonly measured in radial direction, is one of the most important dynamic variables in the dynamic analysis of the precision grinding process [3]. It helps

* Corresponding author.
* Correspondence to: Yong Chen, College of Mechanical Engineering and Automation, Huaqiao University, Xiamen, 361021, China.
*E-mail address:*chenyong@hqu.edu.cn (Y.Chen)

to analyze the brittle-ductile regime transition [4], material elastic-plastic deformation and workpiece surface topography generation [5] during grinding processes. The instantaneous cutting depth of each abrasive grit, is particularly critical for the accurate analysis of the cutting-in and cutting-out behavior of abrasive grits [6-7]，which determines the processing characteristics at different material removal stages, such as rubbing, ploughing and cutting, and governs machining accuracy and surface quality of workpiece. Due to the complex characteristic of different cutting depth of each abrasive grit along the interaction paths between effective working grits and workpiece, the influence of fundamental grinding dynamics and associated surface generation mechanism on the corresponding ground surface quality, especially on surface roughness and surface morphology of workpiece have not fully elaborated from a holistic and systemic perspective.

The influence factors that determine the surface accuracy and quality integrity of workpiece in precision grinding are mainly considered from two aspects [8]. The first one is the exogenous mechanism derived from forced vibration during whole grinding process. Aurich et al discussed main sources of internal and external chatter error and their influences on the surface accuracy of machined workpiece and further presented effective technologies for monitoring and suppressing chatter during the whole machining process to improve surface finish of workpiece [5]. Forced vibration is partly derived from the overall system stiffness features of precision grinding machine tool, Altintas et al described in detail the processing vibration mechanism of systems of machine tool, including machine tool rotary spindle, feeding table movement [7]. Chen et al studied the geometric assembly error of abrasive wheel (such as installation error between abrasive wheel and the motorized spindle system) and its influence on machining vibration during eccentric rotating of abrasive wheel [8]. The second aspect is the endogenous mechanism derived from regenerative vibration during machining process. Huseyin and Ji et al pointed out the regenerative vibration is excited by cutting depth bias as the time-delay effect occurs when adjacent abrasives remove material in the same position of surface waviness [9-10]. As a result, the regenerative vibration is almost unavoidable.

Considering aforementioned comprehensive excitation mechanisms of the exogenous and endogenous vibrations, the instantaneous cutting depth and its distribution in the grinding interaction zone between abrasive grits and workpiece will be significantly different from those conventional studies that utilizes the analytical derivation or the experimental research under a few ideal assumptions of machining conditions. Combined with complex machining dynamics of grinding process, Huseyin et al [9] proposed that the excitation of regenerative vibration was the most important influence factor that had resulted to self-excited vibration machining error. In order to systematically reveal the effect of regenerative vibration mechanism on dynamic characteristics of grinding process, Altintas et al put forward a set of precise dynamics time-delay differential equations, then developed the relevant decoupling algorithm in time domain and frequency domain respectively [7]. Considering the multi-factors influence of regenerative vibration, modal coupling and process damping, Ji et al improved the expression of two-degree-of-freedom dynamics equation of the cutting process by means of full discrete method (FDM) and the stability limit threshold map (SLDs) and model simulation prediction accuracy were verified by experiments [10]. In order to reduce the influence of uneven distribution of abrasive mass on grinding parameters and workpiece surface morphology during grinding, Ding et al proposed an optimization technique of single layer ultra-hard CBN grinding wheel preparation by optimizing the offline / online truing and dressing grinding wheel [11]. Under the conditions of high speed and ultra-high speed grinding process, Li and Sun et al focused on the abrasion behavior of bonded abrasive grits on surface of abrasive wheel, such as the tendency to crumble due to high load or locally spalling due to

insufficient bonding strength [12-13]. Further they put forward the optimization measures of reducing wear between abrasive grits and workpiece. Badger and Ikkache et al analyzed some situations of the eccentric rotation behavior of grinding wheel and studied influence of wheel eccentricity on grinding force, grinding wheel wear and surface topography of workpiece, and further developed a prediction model of surface waviness of workpiece [14-15]. In the investigations mentioned above, the endogenous and exogenous influence on surface finish during precision grinding were analyzed in detail from the aspects of grinding dynamics and experimental procedure, and the corresponding improved analytical models or optimized technologies were presented, which provided useful engineering guide that helped to improve surface morphology of workpiece and product quality. To summarize, it is necessary to develop the analytical model of the instantaneous cutting depth and its distribution characteristic of abrasive grit-workpiece by considering the complex influence mechanisms of forced-vibration and self-excited(regenerative) vibration, which could systematically explain microscopic surface generation in the interaction zone between grits and workpiece and the excitation influence mechanism or the integrated mechanisms influence on transient variables of grinding dynamics, such as grinding force, maximum undeformed chip thickness, specific grinding energy and surface topography etc. Moreover, the conclusions in the paper could help understanding of the final ground surface roughness formation and explaining of the different machining performance between up and down grinding processes.

By applying the simulation technology of full discrete method (FDM), the improved analytical model and relevant simulation model of nonlinear cutting depth of single abrasive grit-workpiece are developed to monitor and control the surface quality and processing accuracy of workpiece based on (a) the complex excitation mechanisms of forced vibration and regenerative vibration, (b) the quantitative analysis of the effect of complex mechanism on dynamics process responses, including cutting depth, grinding force, maximum undeformed chip thickness, specific grinding energy, and (c) the morphological characteristics of workpiece surface.

2 Analytical model of cutting depth in radial direction under the condition of complex excitation mechanism

Some simplified assumptions of grinding kinematics or dynamics are suggested to neglect complex effects of diverse vibration-excitation on grinding process variables. During the actual machining process, it is very difficult to completely "eliminate" the eccentric forced-vibration of the running wheel that will unavoidably affects the cutting behavior [9-10]. A two-degree-of-freedom (2-DOF) and improved grinding kinematics model under the conditions of eccentric rotation of abrasive wheel and regenerative vibration between abrasive grit and workpiece is shown in Fig. 1(a). In the meantime, the cutting trajectory of continuously positioned abrasive grits scratch under regenerative vibration is shown in Fig. 1(b) and the cross-section profile distribution of single abrasive grit scratch is shown in Fig. 1(c). With various hypothesized conical cutting-edge profiles, continuous moving abrasive grits cut in and out workpiece materials at various discrete times creating many small scratches with varying spatial distances, staggered or overlapping. The different sectional shapes and cutting depths are formed on the workpiece surfaces, as shown in Fig. 1 (b), which present the surface topography generation of workpiece with a certain accuracy level [16].

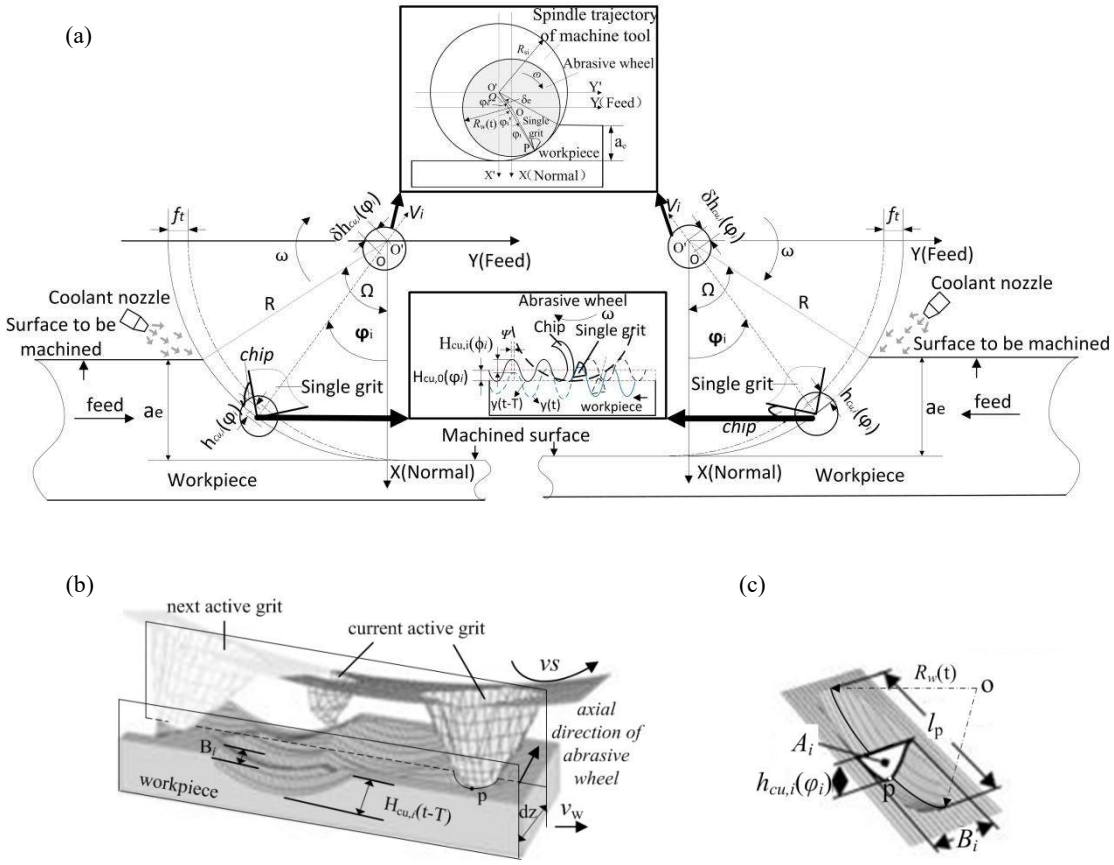

Fig.1. Improved kinematics models with eccentrically rotating wheel and regenerative vibrating behavior. (a) Kinematics model of grinding, (b) Surface micro-topography of workpiece material removed by moving grits with regenerative vibration, (c) Schematics of cross section during single abrasive grit scratching.

According to the different directions of abrasive wheel rotation and workpiece feed, grinding could be divided into two modes, i.e., up-grinding (left) and down- grinding (right), as shown in Fig.1(a). Randomly selecting one abrasive grit *i* positioned on surface of abrasive wheel in the discrete plane with axial spacing *dz*, the abrasive wheel is mounted on the machine tool spindle which rotary center is marked as '*O*'. The study neglects the deformation between abrasive grit and workpiece caused by rubbing or ploughing, so the influence of the difference of up grinding and down grinding could be limited. While in down grinding, the wheel of radius *R* rotates around its own rotary center marked as '*O*' with angular velocity ω (or peripheral velocity v_s) and the workpiece moves in the feed direction velocity v_w, adjacent abrasive grits rotate in each cycle around the machine tool spindle with trajectory of forced vibration according to eccentric rotation and regenerative vibration. Considering the current grit engages at discrete time *t* and previous grit engaged at time *t-T* respectively, the workpiece material is removed with dynamic radial cutting depth $h_{cu,i}(\varphi_i)$ by adjacent abrasive grits at effective grinding radius $R_w(t)$ and $R_w(t\text{-}T)$ in same position *p*, shown in Fig. 1 (a) (middle) , and further surface waviness and morphology of the workpiece with the radial cutting depth $h_{cu,i}(\varphi_i)$ are illustrated in Fig. 1 (b) , the arc cross-section of single scratch shown in Fig. 1 (c) is formed in the longitudinal plane with axial space distance *dz*.

In Fig. 1 (c), the characteristics of single scratch section in abrasive-workpiece interaction area include length l_p, width B_i, maximum cross-sectional area A_i and instantaneous radial cutting depth $h_{cu,i}(\varphi_i)$. Among them, instantaneous radial cutting depth (i.e., scratch depth) of active abrasive grit *i* in

axial section at any cutting trajectory point *p* can be calculated as[8]:

$$h_{\mathbf{cu},i}(\varphi_i) = \Delta h_1(\varphi_i) + \Delta h_2(\varphi_i) + \Delta h_3(\varphi_i) \quad , \qquad 0 \le \varphi_i \le \Omega \quad , \tag{1}$$

In the Equation, the first variable $\Delta h_1(\varphi_i)$ on the right side is the 'static' radial cutting depth. So called 'static' index means it is usually applied to characterize cutting depth regularly deduced in many research papers. The second variable $\Delta h_2(\varphi_i)$ is the 'dynamic' radial cutting depth deviation derived from the eccentric forced vibration of grinding wheel. The third variable $\Delta h_3(\varphi_i)$ is another 'dynamic' radial cutting depth deviation derived from the regeneration vibration of adjacent abrasive grits. $\Delta h_2(\varphi_i)$ and $\Delta h_3(\varphi_i)$ are separately excited by exogenous and endogenous vibration. The angular variable $\varphi_i = \omega t$ is the rotation angle of abrasive grit *i* relative around machine tool spindle rotation center *O'* at discrete time *t*. The static radial cutting depth $\Delta h_1(\varphi_i)$ can be calculated as:

$$\Delta h_1(\varphi_i) = f_t \sin(\varphi_i) \tag{2}$$

While $f_t = \lambda_s \cdot \left({}^{v_w}/_{v_s} \right) = \lambda_s \cdot k_v$ is the feed rate per rotation of the grinding wheel, it represents the maximum undeformed chip feed of single abrasive grit interacting with the surface of workpiece in the grinding contact zone. λ_s is the distance between adjacent active abrasive grits in the same axial cross-section of the grinding wheel, and k_v is the speed ratio between feed speed of workpiece and linear speed of abrasive wheel. If the experiment conditions remain unchanged, the value f_t keeps constant. While abrasive grits are passivated or locally spalled, the value f_t will change linearly with increase of the effective active spacing value λ_s of abrasive grit [12].

The dynamic deviation of radial cutting depth $\Delta h_2(\varphi_i)$ derived from the forced vibration due to the eccentric rotation behavior of abrasive wheel is calculated as:

$$\Delta h_2(\varphi_i) = R_w(t) - R_w(t-T) \tag{3}$$

Here $R_w(t)$ and $R_w(t\text{-}T)$ are the effective grinding radius at current and previous discrete time, as shown in Fig. 1 (a)(top), and can be calculated as :

$$R_w(t) = \sqrt{{R_{si}}^2 + \delta_e^2 - 2R_{si}\delta_e \cos(\theta_s)} \tag{4}$$

Where R_{si} $(i = 1, 2, \ldots n)$ is the effective turning radius of each abrasive grit from machine tool spindle center *O'* to cutting point in arc interaction zone when the cutting depth is a_e, it is calculated as :

$$R_{si} = R + \Lambda_{si} + \delta_e \cos\varphi_{e0i} \tag{5}$$

Where $\Lambda_{si}(i = 1, 2, \ldots n)$ is the protrusion height of abrasive grit *i* on the surface of wheel, which is a characteristic variable that conforms to the Gaussian distribution with the mean value Λ_{savg} and standard deviation σ. The Λ_{savg} value is very close to the corresponding grit abrasive size, so it could be measured by SEM imaging measurement experiment prior to grinding [17]. $\delta_e = \bar{O}O'$ is the eccentricity rotation variable of abrasive wheel due to the limited installation accuracy between abrasive wheel substrate base and machine tool spindle and its value becomes larger with the deterioration of dynamic wheel wear during grinding process. The value can be measured by the offline / online dynamic balance experiments prior to grinding. The limit value applying in conventional precision grinding is 1-3 um to avoid chatter that has great influence on the wheel life and machining accuracy. φ_{e0i} represents the installation position angle of prospective abrasive *i* relative to machine tool spindle center *O'*. When the initial installation position angle between the rotation center *O'* of abrasive wheel substrate base and rotation center *O'* of

machine tool spindle is determined, the value φ_{e0i} can be calculated according to the initial distribution position of the prospective abrasive i on wheel substrate base. So, the radius of wheel substrate base, protrusion height of abrasive grit, initial eccentricity error of wheel and initial installation position of wheel center are determined, the effective rotation radius R_{si} of single active abrasive grit on the surface of abrasive wheel can be calculated accurately.

The variable $\theta_s = \angle PO'O = |\varphi_e - \varphi_i|$ in Equation (4) is rotation angle of active abrasive grits with rotary radius from the rotation position around machine tool spindle center to the one around the eccentricity center of abrasive wheel; $\varphi_e = \varphi_{e0} - \varphi_i$ is the position angle of abrasive wheel center relative to machine tool spindle center.

Substituting above variable into Equation (4), there is:

$$R_w(t) = \sqrt{{R_{si}}^2 + \delta_e^2 - 2R_{si}\delta_e \cos(|\varphi_{e0} - 2\omega t|)} \tag{6}$$

In Equation (1), the variable$\Delta h_3(\varphi_i)$ derived from the regenerative vibration is dynamic deviation of radial cutting depth, which can be calculated as:

$$\Delta h_3(\varphi_i) = (H_{cu,i}(t) - H_{cu,i}(t-T)) \tag{7}$$

Where $H_{cu,i}(t)$, $H_{cu,i}(t\text{-}T)$ are respectively dynamic displacements of the current and previous workpiece in radial direction at instantaneous same position angle φ_i under regenerative vibration conditions[5][18]. Equation (7) is projected to the Cartesian coordinate in Fig. 1(a) as:

$$(H_{cu,i}(t) - H_{cu,i}(t-T)) = （X_{cu,i}(t) - X_{cu,i}(t-T)）\cos\varphi_i + （Y_{cu,i}(t) - Y_{cu,i}(t-T)）\sin\varphi_i \tag{8}$$

The limit value Ω of the radial cut-in angle of abrasive grit shown in Fig. 1 (a) is calculated to determine the effective interaction area of prospective abrasive grit as follows :

$$\Omega = \arccos(1 - \frac{a_e}{R_{si}}) \tag{9}$$

The rotation angle of abrasive grit i is $\phi_i > \Omega$, which means prospective abrasive grit tends to leave from abrasive grit-workpiece interaction area, and the cutting depth turns to zero.

Besides the radial cutting depth, the maximum undeformed chip thickness a_{gmax} is also commonly used to characterize material remove behavior of single abrasive grit and has the influence on other process variables, such as power consumption, surface roughness, grinding force and grinding heat etc. Neglecting elastic deformation of workpiece executed by abrasive grits in interaction zone, the conversion relationship between the maximum undeformed chip thickness a_{gmax} and the radial cutting depth can be expressed as [5] :

$$a_{g\max} = 2\lambda_s \frac{v_w}{v_s}\sqrt{\frac{h_{cu,i}(\varphi_i)}{d_{si}}} = \lambda_s k_v \sqrt{\frac{2h_{cu,i}(\varphi_i)}{R_{si}}} \tag{10}$$

In many previous studies, instantaneous radial cutting depth model of single abrasive grit is simplified to the ‘static’ variable calculated on the basis of the cycloidal trajectory that combined with rotatory motion of active abrasive grits around the machine tool spindle and the feed motion of workpiece. Based on the analysis from Equations. (1), (2), (3) and (7), the model is further improved to be combination with one ‘static’ variable and two ‘dynamic’ variables. The two ‘dynamic’ variables of

cutting depth model consider comprehensive excitation mechanisms with self-excited regenerative vibration and forced vibration from eccentric rotatory of abrasive wheel in accordance with actual installation accuracy. Furthermore, taking many varying factors including the increase of abrasive grit wear and the vibration deterioration of machine tool process system into account, both of 'static' cutting depth affected by the spacing distance between adjacent active abrasive grits and the 'dynamic' cutting depth affected by the eccentricity of abrasive wheel and the regenerative vibration amplitude varies simultaneously with linear or non-linear relationships in real-time. In the meantime, the relevant components, including scratch depth calculated by Equations (2), (3) and (7), the effective cutting radius of abrasive grit calculated by Equation (5) and the maximum undeformed chip thickness calculated by Equation (10) change dynamically. Therefore, the improved dynamics model shown in Fig.1 meets actual machining demands and the calculation accuracy of the relevant variables will be closer to the one in real state.

3. Discrete model of grinding force and specific grinding energy

In Fig. 1(a), while the single abrasive grit i is at cutting-in position, the axial grinding force is negligible because of little effect on the excitation stability and the ground surface quality of workpiece. The instantaneous grinding force executed by grit 'i' in the shear plane dz that is normal to the wheel rotational axis are the resultant of tangential force dF_{ti} and radial force dF_{ri}, which can be calculated as follows [8]:

$$\begin{bmatrix} \mathrm{d}F_{ti}(\varphi_i) \\ \mathrm{d}F_{ri}(\varphi_i) \end{bmatrix} = \begin{bmatrix} K_s \\ c_s K_s \end{bmatrix} \left[v_w / v_s\right]^{2\varepsilon-1} \left[d_{si}\right]^{1-\varepsilon} h_{cu,i}(\varphi_i)\ \mathrm{d}\varphi_i \tag{11}$$

Substituting Equation (1), (2), (3) and (7) into Equation (11), it is calculated as:：

$$\begin{bmatrix} \mathrm{d}F_{ti}(\varphi_i) \\ \mathrm{d}F_{ri}(\varphi_i) \end{bmatrix} = \begin{bmatrix} K_s \\ c_s K_s \end{bmatrix} \left[d_{si}\right]^{1-\varepsilon} \times$$

$$\left(\lambda_s \left[v_w / v_s\right]^{2\varepsilon} \sin(\varphi_i) + \left[v_w / v_s\right]^{2\varepsilon-1} (R_{\mathrm{w}}(t) - R_{\mathrm{w}}(t-\mathrm{T})) + \left[v_w / v_s\right]^{2\varepsilon-1} (H_{\mathrm{cu},i}(t) - H_{\mathrm{cu},i}(t-T))\right) \mathrm{d}\varphi_i$$

$$= \begin{bmatrix} K_s \\ c_s K_s \end{bmatrix} \left[d_{si}\right]^{1-\varepsilon} \left(\lambda_s k_v^{\,2\varepsilon} \sin(\varphi_i) + k_v^{\,2\varepsilon-1} (R_{\mathrm{w}}(t) - R_{\mathrm{w}}(t-\mathrm{T})) + k_v^{\,2\varepsilon-1} (H_{\mathrm{cu},i}(t) - H_{\mathrm{cu},i}(t-T))\right) \mathrm{d}\varphi_i$$

$$= \Delta \mathrm{F}_1(\varphi_i) + \Delta \mathrm{F}_2(\varphi_i) + \Delta \mathrm{F}_3(\varphi_i) \tag{12}$$

where K_s is described as specific grinding force in per unit chip area considering the distribution density, protrusion height and negative rake angle of active abrasive grits, c_s is force ratio between in tangential and radial directions. These variables are also determined by the wheel sharpness, workpiece material property and grinding modes and can be obtained from experimental data. The d_{si} is the effective rotary diameter of single abrasive grit and $h_{cu,i}(\varphi_i)$ is the instantaneous chip thickness as depicted in Equation (1). The constant ε is comprehensive influential coefficient of single grit i friction behavior at the position p and approximately was set as 1 for a pure shear process. Corresponding the static and

dynamic variables in radial cutting depth model, $\Delta F_1(\varphi_i)$, $\Delta F_2(\varphi_i)$ and$\Delta F_3(\varphi_i)$ represent 'static' and 'dynamic' grinding forces considering comprehensive mechanism influences of forced vibration and regenerative vibration respectively.

Moreover, instantaneous specific energy consumption ΔP_{mi} can be calculated by considering adjacent single abrasive grit in removing the material per unit volume of workpiece [19]:

$$\Delta P_{mi} = \frac{10^3 \mathrm{d}F_{ti}(\varphi_i) v_s}{h_{\mathrm{cu},i}(\varphi_i) \times v_w \times B_i} = \frac{10^3 \mathrm{d}F_{ti}(\varphi_i)}{h_{\mathrm{cu},i}(\varphi_i) \times k_v \times B_i} \tag{13}$$

Instantaneous grinding forces calculated in Equation (12) are projected to the Cartesian coordinate system in the normal (X) and feed（Y） directions respectively as:

$$\begin{bmatrix} \mathrm{d}F_{xi} \\ \mathrm{d}F_{yi} \end{bmatrix} = \begin{bmatrix} -\sin\varphi_i & -\cos\varphi_i \\ \cos\varphi_i & -\sin\varphi_i \end{bmatrix} \begin{bmatrix} \mathrm{d}F_{ti}(\varphi_i) \\ \mathrm{d}F_{ri}(\varphi_i) \end{bmatrix} \tag{14}$$

4 Experimental conditions and methods

The experimental study was performed under stable operation conditions on the same precision grinding machine tool (Jones and Shipman 540). The device is shown in Fig.2. The grinding force and surface morphology of workpiece were measured and experimental data analyses were conducted under the conditions of various process parameters, as listed in Table 1. Keeping main grinding parameters unchanged, five groups of grinding experiments were performed while eccentric rotation deviation of abrasive wheel was calibrated to 1 um utilizing one static / dynamic balancer instrument (NHY-2000 - 810A). The data of dynamics variables were evaluated with average data measured in five groups experiments. Resin bonded diamond grinding wheel (diameter of wheel substrate base was 162 mm, the average size of sample grits with fineness number of 100/120 was 0.15 mm, following international standard ANSI-B74-16). The low-carbon steel (EN8) workpiece of size 50×5×50 mm was fixed on feed table of the machine tool. A series of dynamics experiments of down-grinding and up-grinding were performed with single-stroke and repeated-stroke modes. The piezoelectric force sensor (Kistler 9257B) with sampling frequency 50 kHz was mounted to measure grinding force signals in feed direction (movement direction of workpiece) and in normal direction (perpendicular to feed direction). By means of the Charge Amplifier and A / D unit (PMD-1608FS) which measurement channel phase was calibrated prior to grinding and a computer equipped with Graphical Data Analysis software (LABVIEW). The experimental signals were collected into a Signal Analyzer (CSI3005III). Surface roughness of machined workpiece was measured by a Surface Topography Analyzer (TAYLOR HOBSON Surf-6) shown in Fig. 3, and sampling width of workpiece surface was 5 mm. The cross-section characteristics of single micro-slot scratch of workpiece were measured and evaluated by a Laser Confocal Detector (LSM700), and sampling width of workpiece surface is 0.5 mm.

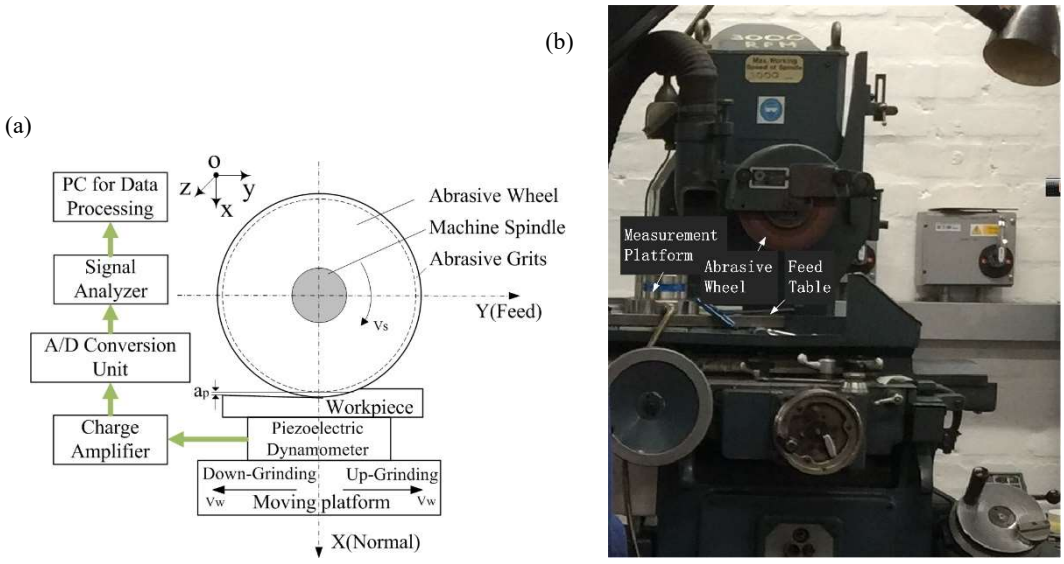

Fig. 2. Experimental instrument of surface grinding dynamics. (a) Experimental diagram, (b) Equipment schematics.

Table 1.

Conditions of dynamics experiments in surface grinding.

Workpiece material	Diameter of abrasive wheel (*mm*)	Fineness No. of grits	Grinding type	Cutting depth of grinding(*um*)
Low-carbon steel(EN8)	162	100-120#	Up grinding or down grinding with single-stroke and repeated-stroke modes	5, 10, 15
Spindle speed(*rpm*)/linear speed of abrasive wheel(*m*/s)		Feed rate of workpiece(*mm/s*)		Additional measures
2880 / 24.4		150, 300		Dry grinding or wet grinding spraying water-based emulsified oil

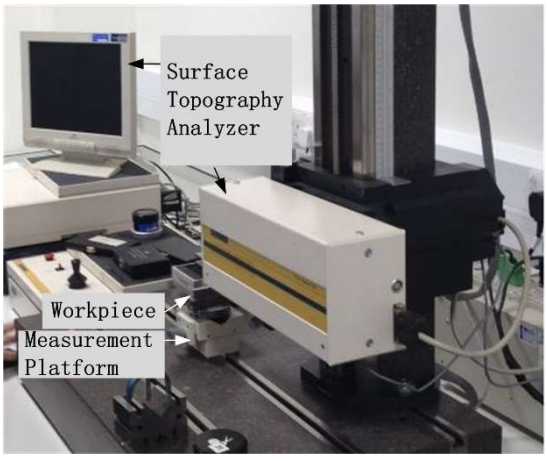

Fig.3. Experimental instrument of surface roughness.

5. Discussion

According to quantitative analysis of relevant theoretical models in a set of Equations (2), (3), (7),

(10), (12) and (13), various grinding process parameters, including grinding modes, speed ratio k_v and total cutting depth a_e, have important influences on process variables, including instantaneous cutting depth, grinding force, specific grinding energy, surface roughness of workpiece and machining accuracy. Compared with some conclusions on grinding dynamics verified in many previous studies [9-10, 20], the complex influence mechanism of regenerative vibration and forced vibration on instantaneous radial cutting depth, scratch characteristics of workpiece surface and final machined surface morphology can be used to evaluate the presented dynamics models with quantitative and comprehensive methods.

5.1 Effect of Grinding mode and Lubrication Cooling Method

According to previous experience and research, it was understood that grinding mode (down grinding or up grinding) together with appropriate lubrication and cooling conditions is crucial to quality improvement of machined surface. As shown in Fig. 4, the lubrication cooling method by means of spraying water-based emulsified oil from cooling nozzle to workpiece with injection pressure of 0.4 MPa. The principle of chip formation process and lubricant flow in the situation where a single active abrasive grit removes workpiece material are illustrated in Fig. 4.

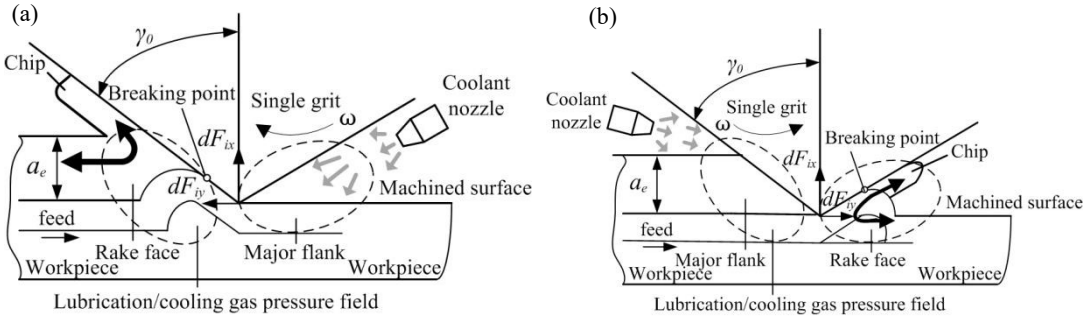

Fig.4 Flow analysis of chip formation under different grinding modes and lubrication cooling conditions. (a) up grinding, (b) down grinding.

With the perspective of the influence of cooling fluid on improvement of machining quality, the fluid mainly plays the role of lubrication, cleaning and cooling in grinding zone. On one hand, grinding coolant helps to form a lubricating film that resists the damage of workpiece surface under the high pressure and high temperature even on presented in the severe friction zone between abrasive grits and workpiece[19]. The lubrication film is also conducive to preventing friction wear of abrasive grit, damping friction appropriately between abrasive wheel and workpiece, and maintaining stable grit spacing λ_s of adjacent active abrasive grits. On the other hand, the coolant takes fine debris of workpiece away, improving wheel pore blockage, promoting self-sharpening of abrasive grits due to rapid cooling of single cutting point of abrasive grit and maintaining sharpness and protrusion height Λ_{si} of abrasive grits, which implies to large radial cutting depth. Meanwhile, it is helpful to rapidly take the heat generated during process away from interaction area and to make temperature of workpiece surface cool down, prevent deterioration of workpiece surface quality.

It is further found that effects of grinding modes, cooling, lubrication and cleaning of coolant on the improvement of machining quality are not completely separated. Combined with analysis of up grinding process shown in Fig. 1 (a) and Fig. 4 (a), it is shown that radial cutting depth of prospective abrasive grit gradually increases from shallow to deep along machining path, which means that instantaneous removing material at current moment starts from original surface generated by previous abrasive grit. At

the beginning of up grinding, radial cutting depth of prospective abrasive grits is relatively small. The material deformation evolves from ploughing phase to chip formation, which results in the elevation of grinding force and temperature. With the increase of cutting depth of the concerned single abrasive grit, the mechanical impact of forced vibration and regeneration vibration on the instantaneous load and the thermal impact in grinding contact zone increase nonlinearly, which destabilize the motion stability of the grits in the high temperature region between abrasive grit and workpiece. When up grinding is finished, the chips are taken away from machined surface of workpiece along the direction of grit rotatory trajectory and the direction of the coolant flushing under high pressure (from right to left shown in Fig. 4(a)), which effectively ensures that machined surface avoid secondary scratch of other new chips. That is why higher quality surface of workpiece is easily obtained in up-grinding.

In contrast with up grinding, radial cutting depth of prospective abrasive grit decreases along cutting path in down grinding. As shown in Fig. 1 (b) and formula (1), when an abrasive grit cuts in material at the critical point in arc interaction zone (i.e. $\varphi_i = \Omega$), the instantaneous radial cutting depth $h(\varphi_i)$ reaches its maximum, which means grinding force and dynamic load of abrasive grits reach maximum. Meanwhile, due to the superposition of vibration impact of prospective abrasive grit, the amplitude of forced vibration and regenerative vibration under comprehensive excitation frequency during high-speed and eccentrically rotating of abrasive wheel spindle tends to be relatively larger at the beginning of grit cut-in during down grinding. The stability of the process is becoming better due to machining vibration calms from strong to steady. As shown in Fig. 4 (b), formed chips will scratch through the machined surface along active direction of abrasive grits and flowing direction of lubricant fluid under high-pressure, which further deteriorates surface quality of machined workpiece.

To verify influence mechanism of chip formation with cutting depth taken by single abrasive grit on surface quality of workpiece, single stroke grinding experiments on conditions of different grinding modes and cutting depth are conducted. Grinding forces in normal and feed directions measured are shown in Fig. 5. Remaining cutting depth of 5um and lubricant conditions, surface roughness and morphological characteristics of workpiece in axial cross-section (in Z direction perpendicular to feed direction of workpiece) are illustrated in Fig. 6 with down grinding and up grinding separately. The sampling area of workpiece surface is 0.7 mm.

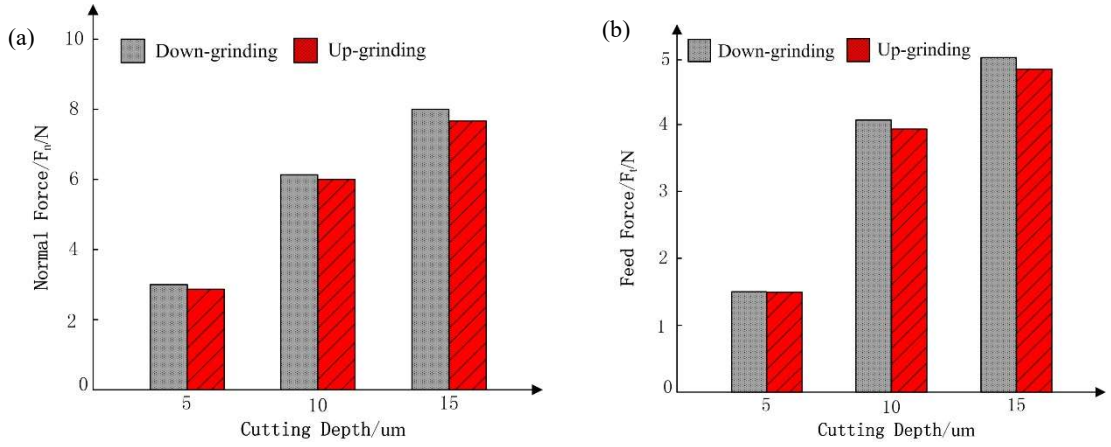

Fig.5 Grinding force with different grinding modes. (a) in normal direction, (b) in feed direction.

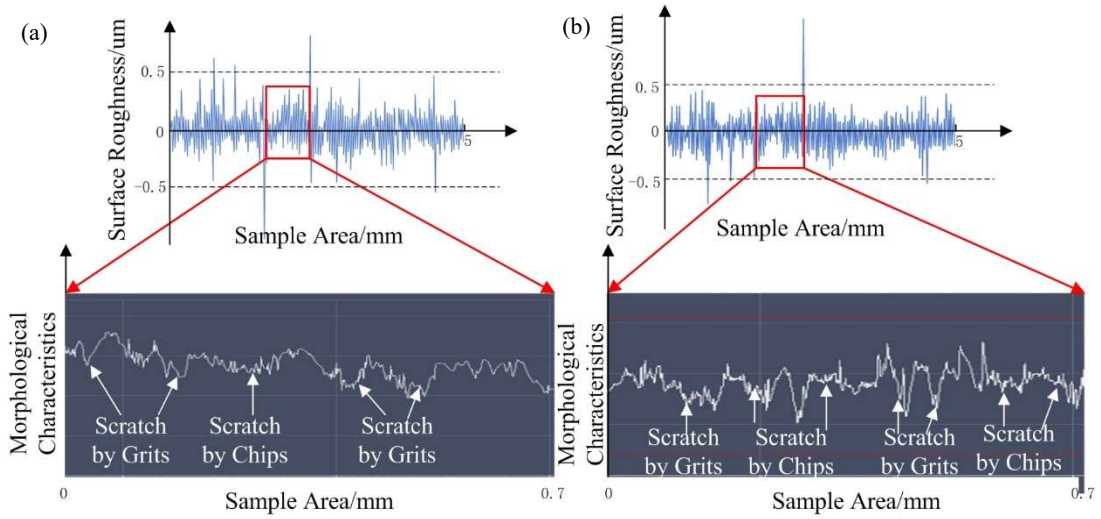

Fig.6 Morphological characteristics of workpiece surface with different grinding modes. (a) Up-grinding, (b) Down-grinding

As shown in Fig. 5, keeping other experimental conditions unchanged in single-stroke grinding, the normal and tangential grinding forces measured in up grinding are 5%–10% less than the corresponding components in down grinding. With the increase of grinding depth, the differences of corresponding forces between up and down grinding increase gradually. The surface scratch distribution and surface roughness of the machined workpiece in up grinding are better than those in down grinding, as shown in Fig. 6, where coolant was applied for both grinding modes. In Fig. 6 (a), the surface morphology of machined workpiece in up grinding is measured and the value of the surface roughness is 0.1991 um. By enlarging the local longitudinal section of workpiece surface profile, it shows that the scratch distribution is uniform as active abrasive grits with various protrusion heights remove material of workpiece, the grinding stability is better, and the fine scratches due to debris is less. In Fig. 6 (b), surface morphology of machined workpiece in down-grinding is measured, the value of the surface roughness is 0.3149 um. It is higher than that in up grinding. The morphological characteristics distribution of the scratches on the workpiece surface is relatively denser, which are mainly resulted from the scratches formed by active abrasive grits with different protrusion heights. Under the influence of superposition effect of instantaneous impact and regenerative vibration during down-grinding process, cutting depth of the scratches in cross-section is further intensified. The fine scratches in down grinding have obviously distributed on the machined surface irregularly, which illustrated the secondary scratching of chips debris and the influence on workpiece surface finish. The measured results actually show the surface roughness of workpiece in up grinding is nearly 37 % higher in comparison with that in down grinding in terms of the reduced average value of surface roughness and fine scratches waviness of machined workpiece.

5.2 Influence analysis of speed ratio(k_v)

According to engineering experiences, if only increasing grinding speed (v_s), but not increasing feed speed of workpiece (v_w) and total cutting depth (a_e), grinding force (especially normal grinding force) should be reduced to a certain extent, specific grinding energy should be correspondingly reduced and higher surface quality of workpiece is obtained. However, the increase of grinding speed leads to increase of power output of machine tool motor, and to result to maximum undeformed chip thickness (a_{gmax}) in

each rotation reduces accordingly, as shown in Formula (10), which means that chip thickness becomes thinner and implies the machining process is not efficient despite on condition of high speed. Therefore, in order to realize grinding process with high efficiency and accuracy, it is necessary to make an analysis of comprehensive influence of speed ratio(k_v) on other process variables, and reveal influence mechanism of these process variables on workpiece surface generation.

The experimental and simulated results of grinding force per unit width in normal and feed directions on conditions of different cutting depths and various speed ratios in down grinding are shown in Fig. 7. Considering the comprehensive excitation influences of forced vibration and self-excited vibration, all force components F_1, F_2 and F_3 represent 'static' force and 'dynamic' force excited by regenerative vibration and forced vibration respectively, their values are obtained from simulation prediction using Formula (12). The variation characteristics of these force components depend on 'static' and 'dynamic' factors of radial cutting depth respectively deduced from Formula (1) to (8). The variation tendency of maximum undeformed chip thickness and specific grinding energy are shown in Fig. 8 and Fig. 9.

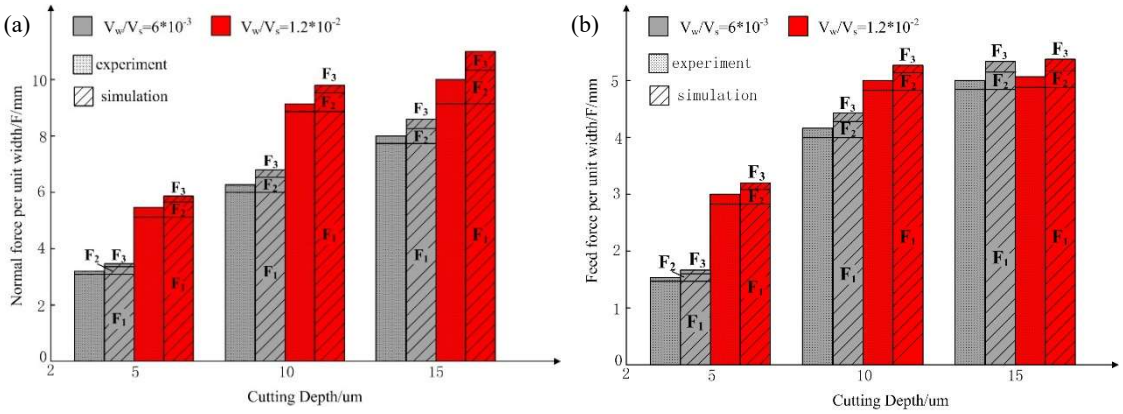

(a) (b)

Fig. 7 Experimental and simulated data of grinding force. (a) in normal direction, (b) in feed direction.

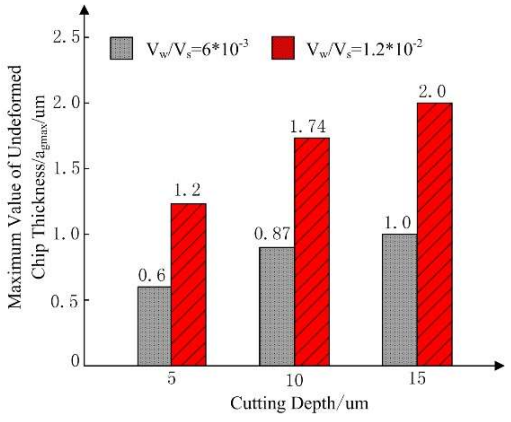

Fig.8 Simulated maximum undeformed chip thickness

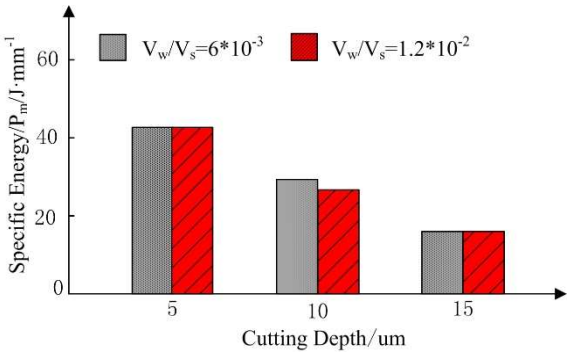

Fig.9 Simulated specific grinding energy

The results in Fig. 7 indicates that the increase of grinding depth results to the increase of each component of radial cutting depth in Formula (1-3) and (7) and further leads to the corresponding increase of total grinding force and its components obtained in Formula (12) and (14) proportionally. The corresponding increasing tendency and their variation proportion will be discussed in detail in section 5.3.

It is shown in Fig. 8 and Fig. 9 that keeping cutting depth unchanged, maximum undeformed chip

thickness calculated in Formulas (10) and (13) increases in almost the same proportion with the increase in speed ratio, while the specific grinding energy nearly remains unchanged with an increase in speed ratio under the combined effects of total grinding force and speed ratio.

The surface morphology of workpiece is measured on the conditions of grinding depth of 10um and speed ratio of 0.006 and 0.012, respectively. The morphological characteristics of scratch section and surface roughness of workpiece are obtained by experimental measurement and simulation prediction are shown in Fig. 10. In Fig.10 (a), (c), (e), surface roughness of workpiece is 0.3894 um at the speed ratio of 0.012, and in Fig.s. 10 (b), (d) and (f), surface roughness of workpiece is 0.2609 um at the speed ratio of 0.006 and surface quality improves nearly 33 % higher than that on the condition of speed ratio of 0.012.

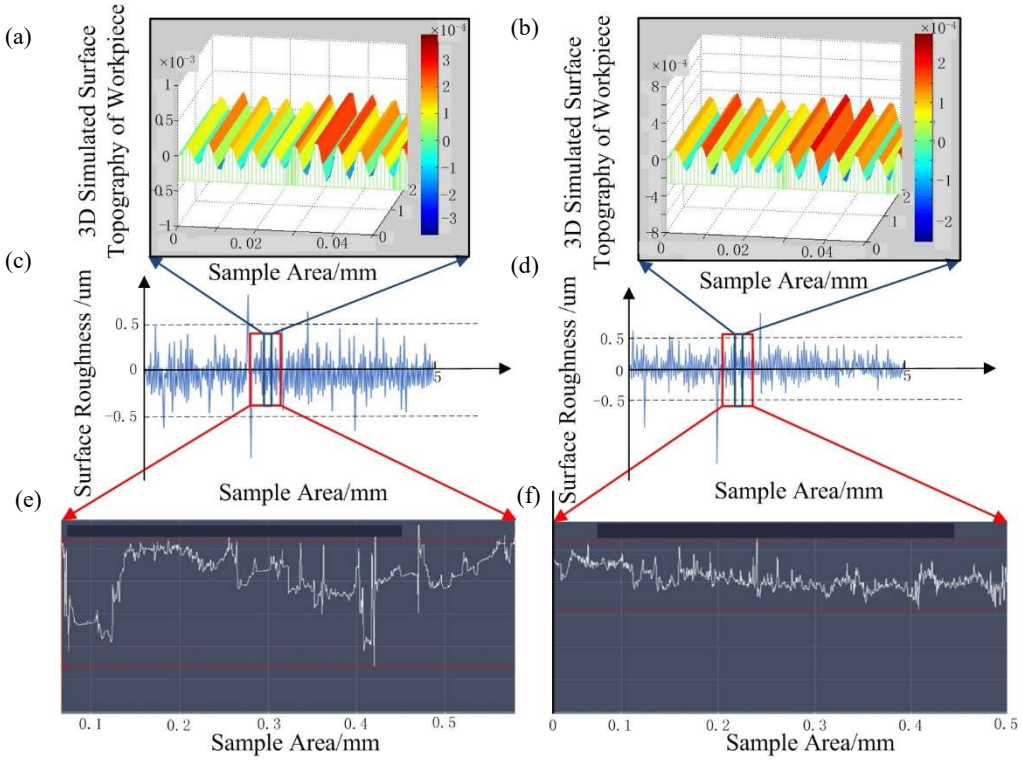

Fig.10. Experimental and simulated data of surface topography of workpiece. (a)(c)(e) Morphological characteristics with value of $V_w/V_s = 1.2*10^{-2}$, (b)(d)(f) Morphological characteristics with value of $V_w/V_s = 6*10^{-3}$

The improvement trend is to be explained that on other process conditions unchanged, while increasing linear speed of abrasive wheel or decreasing feed speed of workpiece by a factor of 2, i.e. speed ratio reduces from 0.012 to 0.006, grinding scratches in cross-section of abrasive grit-workpiece interaction area shown in Fig. 10 (f) are denser than those shown in Fig. 10 (e). It implies that number of abrasive grits conducting to scratch through material in same interval increases, and maximum undeformed chip thickness of single abrasive grit is significantly thinner and slimmer with more uniformly distribution. The conclusion is drawn by means of computer simulation shown in Fig. 8. The single chip thickness in cross-section in Fig. 10 (f) is only one tenth of the average one in Fig. 10 (e). Meanwhile, due to high-speed grinding, both the distance of abrasive grit ploughing and scratching with shorter interval during the chip formation and the pile-up heights formed by plastic ploughing on both sides of grinding grooves reduce. With the reduce of maximum undeformed chip thickness of single abrasive grit, the grinding force and other factors including friction heat generation, workpiece surface

hardening and residual stress are greatly reduced. Under same condition of material removal rate, lower speed ratio helps to improve abrasive wheel life, machining accuracy, process stability and machining efficiency.

In Fig.s 10 (a) and Fig.10 (b), the three-dimensional (3D) simulation prediction of surface topography of machined workpiece with sample distance of 0.5 mm are illustrated. The dynamic distribution of scratches characteristics of adjacent abrasive grits under the conditions of various space distance, unequal protrusion height distribution of grit micro-blade are shown. The variation proportion of surface topography of workpiece are affected by eccentric rotation behavior of abrasive wheel and instantaneous impact of abrasive grits cutting in-out is illustrated visually. The simulation error of surface topography is nearly 10 %.

5.3 Effect analysis of material removal rate

Compared to process parameters, including grinding modes, lubrication and cooling conditions and speed ratio etc, total material removal rate has the greatest impact on process responses, including grinding force, surface roughness of workpiece and process stability. This conclusion has been verified by most experiments. In Fig.s.7 - Fig. 9, while keeping speed ratio k_v constant, total grinding force and its corresponding components of static and dynamic variables and maximum undeformed chip thickness increase with the cutting depth taken by each abrasive grit in experiments and simulation prediction. Their influence is much larger than that from the changes of grinding mode and speed ratio during grinding; and specific grinding energy decreases with the increase of cutting depth of single abrasive grit. Considering coupling effect of forced vibration mechanism and regenerative vibration mechanism, the mean value of total grinding force measured in the experiments is between the static grinding force output (F_1) from the simulation and the sum one accumulating static component(F_1), dynamic component (F_2) excited by forced vibration and dynamic component (F_3) excited by regenerative vibration. The corresponding ratios of static and dynamic components in the simulation of grinding force output under various cutting depths of abrasive grits are shown in Table 2.

Table 2.

Ratios of static and dynamic components of total grinding force

Ratio (%) / Cutting depth (um)	Corresponding ratios of static and dynamic components (%)		
	F_1	F_2	F_3
5	92	5	3
10	89	8	3
15	87	9	4

It is shown in Table 2 that with gradually increased grinding depth, the proportion of dynamic components of grinding force (F_2) excited from forced vibration derived from eccentric rotation of abrasive wheel are twice larger than that excited from regenerative vibration. Combining the effects of F_2 and F_3, their proportion in total grinding force increase with grinding depth as 8 %, 11 % and 13 %, respectively. At the situation of small grinding depth and stable grinding, grinding force increases with cutting depth of single abrasive grit, and the static component of grinding force is nearly 90% of total grinding force. This is why the ‘static’ grinding force is commonly and reasonably regarded as an actual grinding force in most of research. The proportion of the dynamic component of grinding force excited

from the regenerative vibration is so small that its influence is often neglected. With the increase of cutting depth, the coupling influence of forced vibration and regenerative vibration becomes stronger with negative impacts on almost all of dynamics variables in the paper mentioned. Further, on the final machining accuracy and surface finish, even though material removal process remains stable, the dynamical influence takes more attention to present corresponding optimization methods to reduce negative impacts in engineering application.

6. Conclusions

(1) The analytical model of instantaneous cutting depth taken by a single abrasive grit consists of ‘static’ variable derived from material removal mechanism and ‘dynamic’ variables derived from forced vibration and self-excited vibration in a grinding process. These variables have a significant influence on grinding process responses, including grinding force and specific grinding energy and morphological characteristics of workpiece surface.

(2) The total material removal rate has the greatest impact on grinding process responses. With the increase of the cutting depth of single abrasive grit, the stability of grinding process tends to deteriorate under comprehensive excitation from forced vibration and self-excited vibration. The ratio of dynamic grinding force components to total grinding force increase to 13 % while cutting depth of single grit becomes 15um, which further worsens surface topography and machining accuracy of workpiece.

(3) Suitable lubrication and cooling conditions help to obtain high quality machined surface. By means of up grinding, grinding force reduces by 5 % – 10 % and surface roughness of workpiece improve by nearly 37% compared with those in down grinding. Furthermore, evenly distributed scratches on the surface of workpiece created by active abrasive grits make material removal debris has little effect on irregularly secondary scratching in abrasive grit-workpiece interaction zone.

(4) Speed ratio of grinding process has a comprehensive effect on process variables. With an increase in speed ratio in a grinding process, the distribution characteristics of static and dynamic components of grinding force and maximum undeformed chip thickness increase correspondingly, while the specific grinding energy remains almost unchanged. When speed ratio of grinding process deceases to a half, the numbers of active abrasive grits in same interval increase. This leads i) the maximum undeformed chip thickness of single abrasive grit tends to be significantly thinner and slimmer, ii) the depth of surface scratches becomes smaller and the scratches distribute more uniformly, iii) surface roughness of machined workpiece improves by nearly 33%.

Declaration of competing interest

The authors declare no conflict of interest. The funders had no role in the design of the study; in the collection, analyses, or interpretation of data; in the writing of the manuscript; or in the decision to publish the results.

Acknowledgments

This work was supported by the National Natural Science Foundation of China (Grant Nos.

52175404, 51975221).

References

[1] Axinte D, Butler-Smith P, Akgun C, et al. On the influence of single grit micro-geometry on grinding behavior of ductile and brittle materials. Int. J. Mach. Tools Manuf 2013, 74, 12-18.
[2] Liao ZR, Monaca AL, Murray J, Speidel A et al. Surface integrity in metal machining - Part I: Fundamentals of surface characteristics and formation mechanisms. Int. J. Mach. Tools Manuf 2020, 162, 1-51.
[3] Klocke F, Barth S, Mattfeld P. High Performance Grinding. Procedia CIRP. 7th HPC 2016-CIRP Conference on High Performance Cutting 2016, 46, 266-271.
[4] Tian L, Fu Y, Xu J, et al. The influence of speed on material removal mechanism in high speed grinding with single grit. Int. J. Mach. Tools Manuf 2015, 89, 192-201.
[5] Aurich J C, Kirsch B. Kinematic simulation of high-performance grinding for analysis of chip parameters of single grains. CIRP J.Manuf. Sci. Tech 2012, 5, 164-174.
[6] Li C, Duan J, Zhang X, et al,. Grinding performance integrated experimental evaluation on alumina ceramics with leaf-vein bionic grinding wheel. Int.J.Adv. Manuf. Tech 2022, 121, 2525-2537.
[7] Altintas Y, Weck M. Chatter stability of metal cutting and grinding. Annals.CIRP Manuf.Tech 2004, 53, 619-642.
[8] Chen Y, Chen X, Xu XP, Yu G,. Quantitative impacts of regenerative vibration and abrasive wheel eccentricity on surface grinding dynamic performance. Int.J.Adv. Manuf. Tech 2018, 96, 2271-2283.
[9] Huseyin C, Erdem O, Neil DS,. Can mode coupling chatter happen in milling? Int. J. Mach. Tools Manuf 2021, 165, 1-13.
[10] Ji YJ, Wang XB, Liu ZB, Wang HJ, Jiao L, Zhang L, Huang T. Milling stability prediction with simultaneously considering the multiple factors coupling effects—regenerative effect, mode coupling, and process damping. Int. J. Adv. Manuf. Tech 2018, 97, 2509-2527.
[11] Ding WF, Barbara L, Zhu YJ, Li Z, Fu YC et al. Review on monolayer CBN superabrasive wheels for grinding metallic materials. Chinese J. Aero 2017. 30, 109-134.
[12] Li XK, Wolf S, Zhu TX, Zhi G, Rong YM. Modelling and analysis of the bonding mechanism of CBN grains for electroplated superabrasive tools—part 1: introduction and application of a novel approach for determining the bonding force and the failure modes. Int.J.Adv. Manuf. Tech 2015, 76, 2051-2058.
[13] Sun XF, Yao P, Qu SS, Yu SM et al. Material properties and machining characteristics under high strain rate in ultra-precision and ultra-high-speed machining process: a review. Int.J.Adv. Manuf. Tech 2022, 120, 7011-7042.
[14] Badger J, Murphy S, O'Donnell G. The effect of wheel eccentricity and run-out on grinding forces, waviness, wheel wear and chatter. Int. J. Mach. Tools Manuf 2011, 51, 766-774.
[15] Ikkache K, Chellil A, Lecheb S, Mechakra H. Dynamic modeling of milling and effect of tool path on machining stability. Int. J. Adv. Manuf. Tech 2022, 121,1769-1783.
[16] Wang B, Liu ZQ, Cai YK, Luo XC et al. Advancements in material removal mechanism and surface integrity of high speed metal cutting: A review. Int. J. Mach. Tools Manuf 2021, 166,1-13.
[17] Zhang YZ, Fang CF, Huang GQ, Xu XP. Modeling and simulation of the distribution of undeformed chip thicknesses in surface grinding. Int. J. Mach. Tools Manuf 2018, 127, 14-17.
[18] Aurich JC, Kirsch B. Improved coolant supply through slotted grinding wheel. CIRP Annals – Manuf. Tech 2013, 62, 363-366.
[19] Rasim M, Mattdeld P, Klocke F. Analysis of the grain shape influence on the chip formation in grinding. J. Mater. Processing. Tech 2015, 226, 60-68.
[20] Wang XZ, Liu QY, Zheng YH, Xing W, Wang MH. A grinding force prediction model with random distribution of abrasive grains: considering material removal and undeformed chips. Int. J. Adv. Manuf. Tech 2022, 120, 7219-7233.